

UNCLASSIFIED

Defense Technical Information Center
Compilation Part Notice

ADP013145

TITLE: Long Wavelength Quantum Dot Lasers on GaAs Substrates

DISTRIBUTION: Approved for public release, distribution unlimited

Availability: Hard copy only.

This paper is part of the following report:

TITLE: Nanostructures: Physics and Technology International Symposium
[8th] Held in St. Petersburg, Russia on June 19-23, 2000 Proceedings

To order the complete compilation report, use: ADA407315

The component part is provided here to allow users access to individually authored sections of proceedings, annals, symposia, etc. However, the component should be considered within the context of the overall compilation report and not as a stand-alone technical report.

The following component part numbers comprise the compilation report:

ADP013002 thru ADP013146

UNCLASSIFIED

Long wavelength quantum dot lasers on GaAs substrates

V. M. Ustinov[†], *A. E. Zhukov*[†], *A. R. Kovsh*[†], *S. S. Mikhrin*[†], *N. A. Maleev*[†],
B. V. Volovik[†], *Yu. G. Musikhin*[†], *Yu. M. Shernyakov*[†], *E. Yu. Kondrat'eva*[†],
M. V. Maximov[†], *A. F. Tsatsul'nikov*[†], *N. N. Ledentsov*[†], *Zh. I. Alferov*[†],
J. A. Lott[‡] and *D. Bimberg*[§]

[†] Ioffe Physico-Technical Institute, St Petersburg, Russia

[‡] Air Force Institute of Technology, Wright-Patterson Air Force Base, OH, USA

[§] Technische Universität Berlin, D-10623 Berlin, Germany

Abstract. We study $1.3 \mu\text{m}$ diode lasers based on self-organized InAs quantum dots grown by MBE on GaAs substrates. Overgrowing the InAs quantum dot array with thin InGaAs layer allows us to achieve $1.3 \mu\text{m}$ emission and keep sufficiently high surface density of quantum dots. Using transmission electron microscopy we show that the main reason for the long wavelength PL shift in InAs/InGaAs quantum dots is non-uniform distribution of In in InGaAs leading to the increase in effective volume of a quantum dot. Long stripe lasers showed low threshold current density ($<100 \text{ A/cm}^2$), high differential efficiency ($>50\%$), and low internal loss ($\sim 1-2 \text{ cm}^{-1}$). Maximum output power for wide stripe lasers was as high as 2.7 W and for single-mode devices 110 mW . The lasing wavelength for VCSELs was $1.28 \mu\text{m}$. The threshold current for the device with the $12 \mu\text{m}$ apperture was 1.8 mA . The output power of 220 mW at drive current of 2.4 mA was observed under pulsed mode.

Introduction

Diode lasers based on InGaAsP/InP heterostructures emitting at 1.3 and $1.55 \mu\text{m}$ are currently widely used in fiber optical communication systems. These systems are mainly used for long-distance data transmission whereas their application in local networks is limited due to the lack of inexpensive light emitters. Two factors mainly lead to the high cost of the InGaAsP/InP lasers. They are: strong temperature dependence of threshold current density due to small conduction band discontinuity and weak variation of refractive index in InGaAsP system making the synthesis of the VCSEL structure in a single growth run hardly possible. The fabrication of the $1.3 \mu\text{m}$ light emitters on GaAs substrates will allow to overcome those problems and also to avoid the use of expensive InP substrates of inferior quality as compared to that of GaAs.

The increase in emission wavelength from InGaAs/GaAs quantum wells is limited to $1.2 \mu\text{m}$ due to the limitations of pseudomorphic growth. InGaAsN/GaAs quantum wells [1] and InAs/GaAs quantum dots [2] are currently considered as the most promising candidates for increasing the emission wavelength from GaAs based heterostructures. In the present work we show that the emission wavelength of the InAs/GaAs quantum dot heterostructures can be increased to $1.3 \mu\text{m}$ and low-threshold diode lasers with high output power can be realized on their basis.

1. Formation of the InAs quantum dots emitting at $1.3 \mu\text{m}$

InAs/GaAs quantum dot heterostructures were synthesized by molecular beam epitaxy (MBE) *in situ* at the initial stages of strained layer heteroepitaxy via Stranski–Krastanow

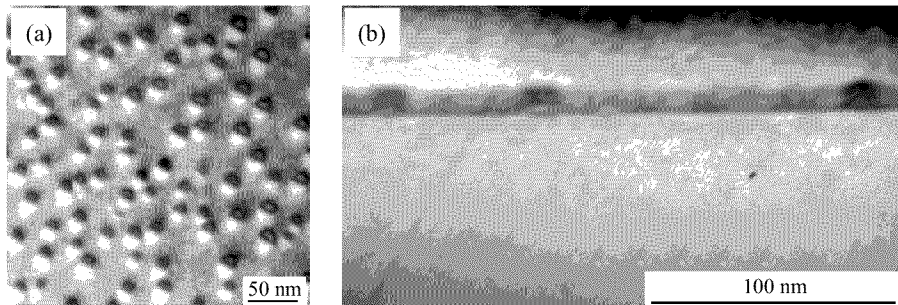


Fig. 1. Plan-view (a) and cross-section (b) TEM images of single plane of InAs quantum dots covered by 5-nm thick $\text{In}_{0.15}\text{Ga}_{0.85}\text{As}$ QW.

growth mode [2]. We have shown earlier that the maximum emission wavelength which can be observed from the InAs/GaAs quantum dot ensemble upon increasing the effective deposition thickness of InAs is $1.24 \mu\text{m}$ at 300 K [3]. Alternative deposition of In, Ga, and As fluxes leads to the formation of larger InAs quantum islands as compared to the usual quantum dots obtained by conventional MBE. This result allowed the authors of [4] to realize $1.3 \mu\text{m}$ lasing from InAs quantum dots on GaAs substrate. However, in this case the surface density of quantum dots is low ($\sim 1.3 \times 10^{10} \text{ cm}^{-2}$), and the problem of insufficient gain forces the authors to use extremely long laser diodes or highly reflective coatings which leads to low differential efficiency. In the present work we use the overgrowth of the InAs quantum dot ensemble by a thin $\text{In}_x\text{Ga}_{1-x}\text{As}$ layer [5]. TEM image shows that in this case the surface density of quantum dots is about $5 \times 10^{10} \text{ cm}^{-2}$, Fig. 1(a). Both the increase in the effective thickness of deposited InAs (QInAs) and the increase in the InAs mole fraction x in the $\text{In}_x\text{Ga}_{1-x}\text{As}$ ternary leads to gradual increase in the emission wavelength which can achieve $1.3 \mu\text{m}$ at certain values of Q_{InAs} and x [6], Fig. 2(a). Figure 2(b) shows characteristic photoluminescence (PL) spectra of InAs/ $\text{In}_x\text{Ga}_{1-x}\text{As}$ quantum dots. This figure also shows that we observe the red shift of the PL line even when we overgrow InAs quantum dots with the $\text{In}_x\text{Al}_y\text{Ga}_{1-x-y}\text{As}$ quaternary whose band-gap is approximately equal to that of GaAs. This unexpected result was explained after studying the cross-section TEM images of the structures, Fig. 1(b). This image shows the characteristic

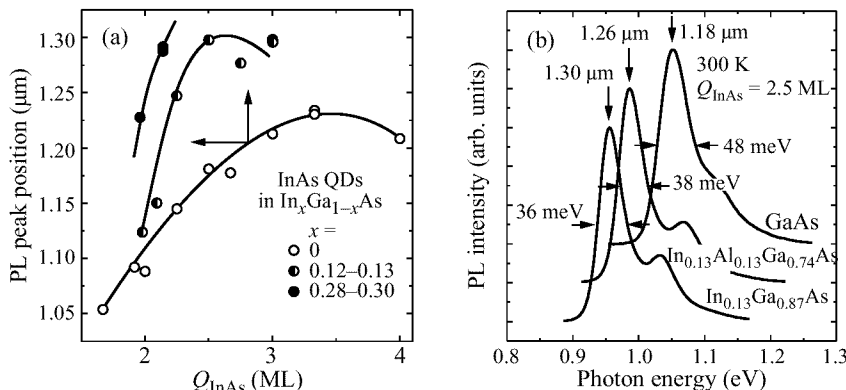


Fig. 2. (a) Dependence of the PL peak position (at room temperature) on the effective thickness of InAs QD plane covered by InGaAs QW of various InAs mole fraction; (b) PL spectra of 2.5-ML InAs QDs covered by various materials.

increase in dark contrast just above the InAs islands which is due to local nonuniformities in the InAs distribution in the InGaAs ternary. As the result, the effective volume of the InAs islands is increased which leads to the long wavelength shift of the PL line. The characteristic PL spectrum (Fig. 2(b)) consists of two features, the main peak is due to the ground state emission and the second (shorter wavelength peak) is due to the excited state quantum dot emission. We should note that the InAs/InGaAs quantum dot structures are characterized by high indium content which could potentially lead to strain relaxation with the formation of misfit dislocations. Therefore, we have minimized the overall In content in the structure keeping $1.3 \mu\text{m}$ emission. We have found that in this case the structures demonstrate maximum PL intensity indicating the lowest defect concentration [6].

The problem of gain saturation characteristic for quantum dot lasers [7] leads to the use of multi-plane quantum dot structures in the active area of quantum dot lasers. We have found that in the case of $1.3 \mu\text{m}$ InAs quantum dots the use of thick ($>20 \text{ nm}$) GaAs spacers between quantum dot sheets allows us to avoid misfit dislocations and to keep high luminescence intensity.

2. InAs/InGaAs $1.3 \mu\text{m}$ quantum dot lasers

The structures for diode lasers studied in the present work were grown by MBE and the quantum dot active region was placed into GRINSCH AlGaAs/GaAs structure with graded waveguide. Si or Be doped $1.2 \mu\text{m}$ Al_{0.8}Ga_{0.2}As layers were used as emitters. The thickness of the waveguide layer was $0.4 \mu\text{m}$. InAs/In_xGa_{1-x}As quantum dots consisted of 2 ML of InAs and 5 nm of In_{0.15}Ga_{0.85}As. The GaAs spacer thickness between quantum dot planes was 30 nm. Laser characteristics were studied as a function of the number of quantum dot sheets. All structures demonstrated luminescence in the $1.25\text{--}1.29 \mu\text{m}$ range. Broad area (100 and $200 \mu\text{m}$ wide) stripe lasers with various cavity lengths were studied under pulsed mode. CW characteristics were measured after mounting the diode p-side down on a copper heat sink. Narrow ($7 \mu\text{m}$) stripes were formed to study the single mode operation.

2.1. Threshold characteristics

It is well known that, to have ground state lasing, the following expression should be valid:

$$\alpha_i + \frac{1}{2L} \ln \left(\frac{1}{R_1 R_2} \right) \leq g^{\text{sat}} \quad (1)$$

here α_i is internal loss, $R_{1,2}$ are mirror reflective indexes, L is cavity length, g^{sat} is saturated gain on the ground state. Important problem for quantum dot lasers is relatively low saturated gain due to a finite surface density of quantum dots and their size dispersion [7]. As the result, in our experiments we failed to realize ground state lasing for single-sheet quantum dot structure. Ground-state lasing at $1.25 \mu\text{m}$ was observed for three-sheet quantum dot laser. The threshold current density as low as 65 A/cm^2 was measured on the four-cleaved sample. Characteristic temperature T_0 was 150 K up to 310 K and then decreased to 50 K presumably due to the population of excited states. Stripe lasers demonstrated differential efficiency of 55% and low internal loss (1.5 cm^{-1}). Internal quantum efficiency was estimated as 70%, (Fig. 3). Figure 3 also shows lasing wavelength as a function of the cavity length. In the $2\text{--}1.2 \text{ mm}$ range ground state lasing is observed ($\lambda \sim 1.25 \mu\text{m}$) and J_{th} increases only slightly. However, at $L \sim 1 \text{ mm}$ lasing jumps from the ground to excited state ($\lambda = 1.17 \mu\text{m}$) and threshold current density is abruptly increased. We attribute this effect to the gain saturation at the ground state. In this case mirror losses are increased with the decrease in the cavity length and finally the overall

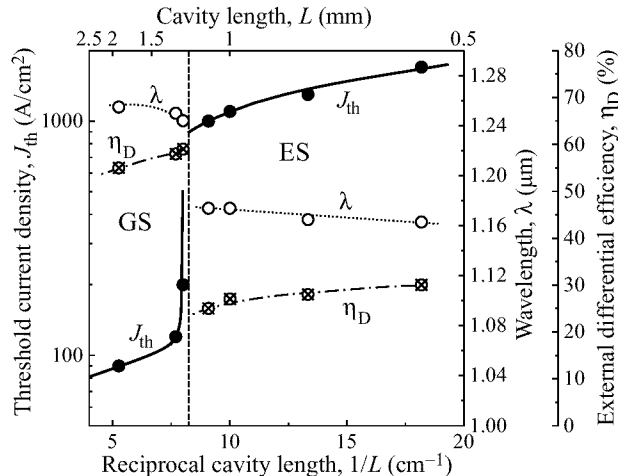


Fig. 3. Cavity length dependence of the threshold current density (solid circles), lasing wavelength (open circles) and external differential efficiency (\times -centered circles).

losses become more than the saturated gain at the ground state. The excited state can accumulate more carriers than the ground state due to the degeneration and, therefore, is characterized by higher g^{sat} and transparency current density. As the result, lasing proceeds via excited state and the threshold current density is increased. Based on the experimental data given above we estimated the value of saturated gain per the quantum dot layer as 4 cm^{-1} . From this result it follows that, to achieve ground state lasing from the short ($400\text{--}500 \mu\text{m}$) diodes, one has to use multi-plane quantum dot structures in the active region of a diode laser. In the present work we observed $1.29 \mu\text{m}$ ground state lasing from the 10-sheet InAs/InGaAs quantum dot laser.

2.2. Power characteristics

High differential quantum efficiency and low internal loss allowed us to demonstrate room temperature CW operation of a quantum dot laser for the structure containing three planes of quantum dots. Broad area laser diodes with the stripe width $100\text{--}200 \mu\text{m}$ showed high output power $1.9\text{--}2.7 \text{ W}$ (output power density $19\text{--}13.5 \text{ mW}/\mu\text{m}$) at 17°C and was limited by thermal roll-over, Fig. 4. Maximum conversion efficiency was 25%. The lasing wavelength at maximum output power was $1.28 \mu\text{m}$ due to the overheating of the active region.

2.3. Single-mode operation

Broad area lasers demonstrated above give multiple mode radiation. However, fiber optical communication systems require single-mode devices. In the present work we studied single-mode devices by fabricating $7\text{-}\mu\text{m}$ wide stripes from the 3-QD-plane structure. Figure 5 shows output power vs pumping current for the 2-mm cavity laser. Threshold current was 60 mA and differential efficiency 37% . The shapes of the far-field patterns for the output power less than 110 mW are close to gaussians which is indicative of a spatially single-mode operation. Further increasing the pumping current leads to the formation of the mixed mode accompanied by the decrease in the output power.

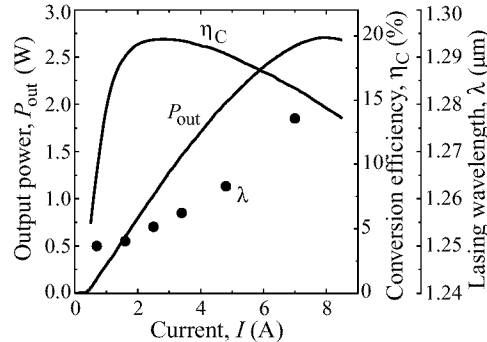


Fig. 4. Output power, lasing wavelength, and power conversion efficiency as function of drive current for 100- μm -wide diode laser.

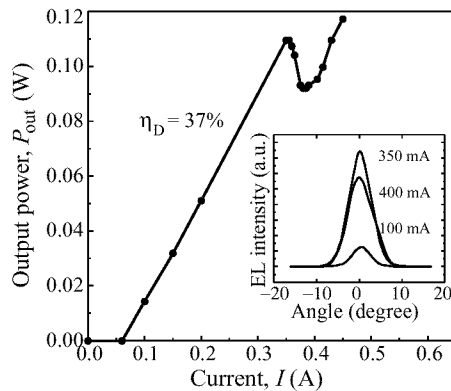


Fig. 5. Output power and lateral far field pattern (insert) as function of drive current for 7- μm -wide ridge waveguide diode laser.

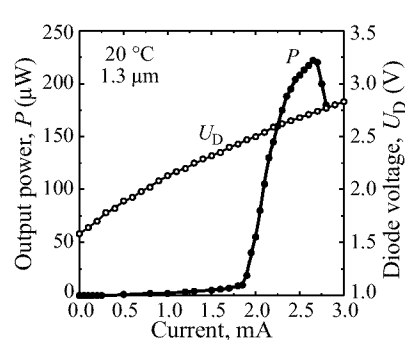


Fig. 6. Output power and diode voltage vs drive current for 12 \times 12- μm^2 Al-oxidized VCSEL.

3. VCSELs

In the present work the VCSEL structure was fabricated by placing the 1.3 μm InAs/InGaAs quantum dot layers into a λ GaAs cavity which was inside the optical cavity formed by AlO/GaAs Bragg mirrors [8]. The AlO layers and the current aperture were formed by selective wet oxidation. Current injection is provided via intra-cavity contacts. The structure showed room temperature lasing at 1.28 μm . The threshold current density for the 12 μm aperture device was ~ 1.5 kA/cm 2 ($I_{th} = 1.8$ mA). The maximum output power under pulsed mode was 220 μW with the external differential of 46%, Fig. 6. To the best of our knowledge this is the longest wavelength current injection VCSEL on a GaAs substrate reported to date.

4. Conclusion

Quantum dot diode lasers emitting in the 1.3 μm range grown by MBE on GaAs substrates have been realized. They showed low threshold current density, high differential efficiency, high output power and single-mode operation. Some characteristics approached to that of the InP based 1.3 μm lasers or even exceed them. In combination with the first data on

the $1.28 \mu\text{m}$ GaAs based VCSEL these results are very promising for applications in fiber optical communication systems.

Acknowledgements

This work is supported by Russian Foundation for Basic Research (grant 00-02-17039), Program of the Ministry of Science and Technology of Russia “Physics of Solid State Nanostructures” (projects 99-2014), and INTAS.

References

- [1] M. Kondow, K. Uomi, A. Niwa, T. Kitatani, S. Watahiki and Y. Yazawa, *Jpn. J. Appl. Phys.* **35**, 1273 (1996).
- [2] D. Bimberg, M. Grundmann and N. N. Ledentsov, *Quantum Dot Heterostructures*, Chichester: Wiley 1999.
- [3] A. Yu. Egorov, A. E. Zhukov, P. S. Kop'ev, N. N. Ledentsov, M. V. Maksimov, V. M. Ustinov, A. F. Tsatsul'nikov, Zh. I. Alferov, Zh. I. Fedorov and D. Bimberg, *Semiconductors* **30**, 707 (1996).
- [4] G. Park, O. B. Shchekin, S. Csutak, D. L. Huffaker and D. G. Deppe, *Appl. Phys. Lett.* **75**, 3267 (1999).
- [5] V. M. Ustinov, *et al.*, *Appl. Phys. Lett.* **74**, 2815 (1999).
- [6] V. M. Ustinov, *et al.*, *Microelectronics J.* **31**, 1 (2000).
- [7] A. E. Zhukov, *et al.*, *Semicond. Sci. Technol.* **14**, 118 (1999).
- [8] J. A. Lott, N. N. Ledentsov, V. M. Ustinov, A. Yu. Egorov, A. E. Zhukov, P. S. Kop'ev, Zh. I. Alferov and D. Bimberg, *Electron. Lett.* **33**, 1150 (1997).